JACS
JOURNAL OF THE AMERICAN CHEMICAL SOCIETY

COMMUNICATION

pubs.acs.org/JACS

# Oxygen-Aided Synthesis of Polycrystalline Graphene on Silicon Dioxide Substrates

Jianyi Chen, Yugeng Wen, Yunlong Guo, Bin Wu, Liping Huang, Yunzhou Xue, Dechao Geng, Dong Wang, Gui Yu, and Yunqi Liu*

Beijing National Laboratory for Molecular Sciences, Institute of Chemistry, Chinese Academy of Sciences, Beijing 100190, P. R. China

Supporting Information

**ABSTRACT:** We report the metal-catalyst-free synthesis of high-quality polycrystalline graphene on dielectric substrates [silicon dioxide ($SiO_2$) or quartz] using an oxygen-aided chemical vapor deposition (CVD) process. The growth was carried out using a CVD system at atmospheric pressure. After high-temperature activation of the growth substrates in air, high-quality polycrystalline graphene is subsequently grown on $SiO_2$ by utilizing the oxygen-based nucleation sites. The growth mechanism is analogous to that of growth for single-walled carbon nanotubes. Graphene-modified $SiO_2$ substrates can be directly used in transparent conducting films and field-effect devices. The carrier mobilities are about 531 $cm^2 V^{-1} s^{-1}$ in air and 472 $cm^2 V^{-1} s^{-1}$ in $N_2$, which are close to that of metal-catalyzed polycrystalline graphene. The method avoids the need for either a metal catalyst or a complicated and skilled postgrowth transfer process and is compatible with current silicon processing techniques.

Graphene is currently the most promising potential successor to silicon for use in next-generation electronic devices because of its fascinating physical properties.[1] In an attempt to fabricate samples of graphene suitable for real-world applications, many approaches have been studied, including mechanical cleavage,[1] epitaxial techniques,[2] chemical exfoliation,[3] and chemical vapor deposition (CVD).[4] Among them, there have been rapid recent advances in the use of metal-catalyzed CVD processes for large-scale synthesis, and large-area graphene films have been successfully grown on Ni and Cu foils.[5,6] It is widely believed that the presence of metals is indispensable for the growth of high-quality graphene, as almost all the CVD methods reported to date rely on metal-catalyzed growth. As a result, complicated and skilled postgrowth techniques have to be employed to remove these metal catalysts and transfer the graphene to the type of dielectric substrate ($SiO_2$/Si or quartz) required for use in practical electronic devices. In many cases, the transfer process results in loss of material, and it is difficult, if not impossible, to avoid contamination, wrinkling, and breakage of the samples. Although much work has also been done to explore the catalyst-free growth of graphene on dielectric substrates,[7−9] nanocrystalline graphene and its lower properties have caught less interest. On the other hand, nanosized $SiO_2$ particles have been used to grow single-walled carbon nanotubes (SWCNTs).[10,11] Here we describe a metal-catalyst-free CVD method for the direct synthesis of high-quality polycrystalline graphene on silicon wafers with a layer of $SiO_2$ ($SiO_2$/Si) and on quartz. One of the major benefits of our method is that it can utilize the oxygen-based nucleation sites for high-quality graphene growth, avoiding the need for either a metal catalyst or a complicated and skilled postgrowth transfer process.

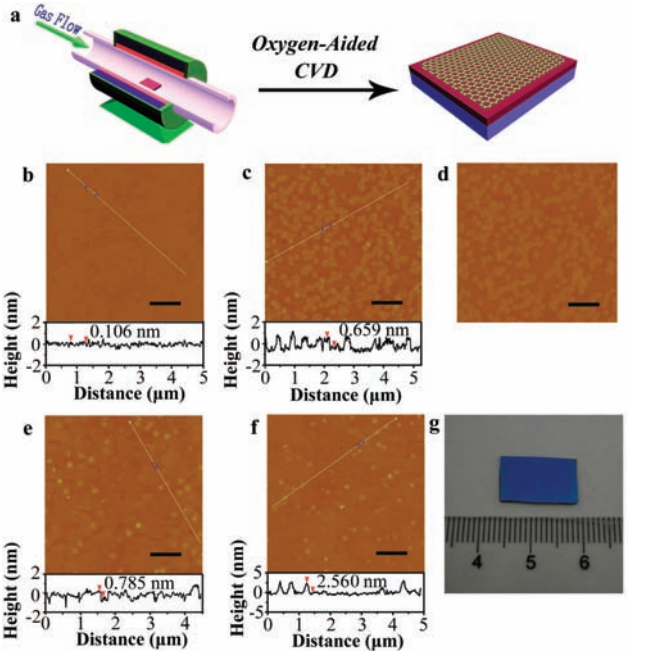


**Figure 1.** Synthesis process and morphological changes of graphene on $SiO_2$/Si substrates. (a) Schematic diagram of the oxygen-aided CVD growth of graphene on a $SiO_2$/Si substrate. (b) Initial surface of the $SiO_2$/Si substrate, characterized by a uniform flat surface. (c) AFM height image of graphene sheets with a thickness of ~0.659 nm. (d) AFM phase image of graphene sheets. (e) AFM image of 2D interconnected graphene networks. (f) AFM image of continuous graphene films. (g) Photograph of a graphene film on $SiO_2$/Si substrate. The edge was removed using adhesive tape. Scale bar = 1 $\mu$m.

As described in Figure 1a, $SiO_2$/Si substrates were directly placed in a quartz tube mounted inside a high-temperature furnace (1100 °C) for graphene synthesis. In contrast to the typical procedure for graphene growth, we annealed the $SiO_2$/Si substrates at 800 °C in flowing air before growth to remove any organic residues and activate the growth sites (Figure S1 in the

**Received:** July 8, 2011
**Published:** October 11, 2011

  

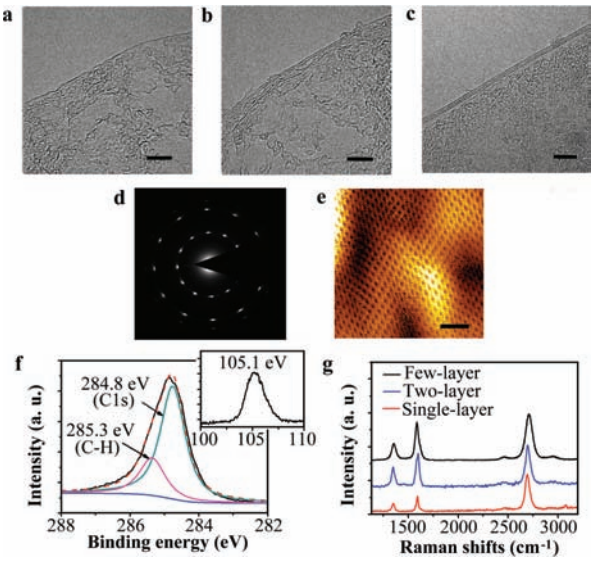


**Figure 2.** Analyses of graphene films produced by oxygen-aided CVD. (a−c) HRTEM images of (a) monolayer, (b) two-layer, and (c) three-layer graphene. Scale bars = 5 nm. (d) SAED pattern of graphene, showing two sets of hexagonal patterns. (e) STM image ($I_t$ = 0.5 nA, $V_s$ = 25 mV) of the graphene honeycomb lattice. Scale bar = 1 nm. (f) C 1s and (inset) Si 2p XPS spectra of a graphene film. (g) Raman spectra (514 nm laser wavelength) of a graphene film.

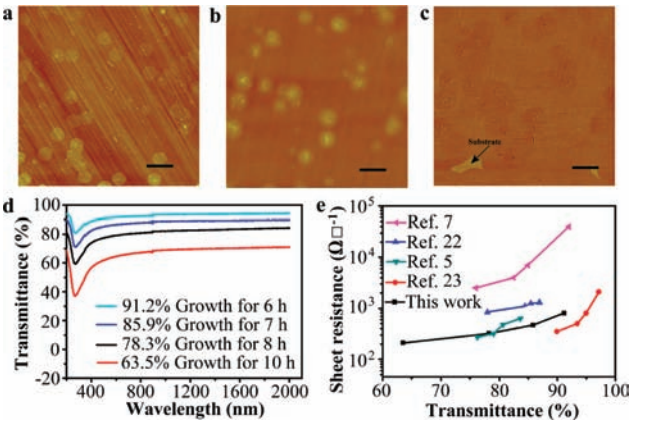


**Figure 3.** Optical and electrical properties of oxygen-aided graphene film on quartz. (a) AFM height image of discrete graphene sheets after a 2 h growth. Scale bar = 1 $\mu$m. (b) AFM height image of graphene film after a 6 h growth. Scale bar = 1 $\mu$m. (c) AFM phase image of graphene film. Scale bar = 1 $\mu$m. (d) Transmittance spectra of oxygen-aided graphene films on quartz. (e) Comparison of the properties of transparent conductive films obtained in this work and other examples in the literature.

Supporting Information). Density functional theory calculations[11,12] have revealed that the presence of oxygen can enhance the adsorption of hydrocarbons on $SiO_2$. Atomic force microscopy (AFM) images of the $SiO_2$/Si surface topography before and after growth are shown in Figure 1b−f. The commercial $SiO_2$/Si chip used as the growth substrate is characterized by a uniform flat surface (Figure 1b). After exposure to the flowing reaction gas mixture ($CH_4$:$H_2$:Ar = 14:50:65 sccm) for 3 h, the $SiO_2$/Si surface became covered with monolayer graphene islands (Figure 1c,d). The graphene phase image (Figure 1d) reveals a clear contrast with the $SiO_2$/Si substrate, and the thickness of graphene sheets is ∼0.659 nm (Figure 1c). The size and number of the graphene sheets can easily be controlled by changing the carbon flow, deposition temperature, or growth time (Figure S2). Continued deposition enlarges the size of graphene sheets, and many nearest-neighbor graphene sheets link together, initially resulting in 2D interconnected graphene networks (growth time 7 h; Figure 1e) and subsequently continuous graphene films (growth time 8 h; Figure 1f,g), which contain a number of islands of greater thickness. The height profile taken along the white line in Figure 1f shows a step height of ∼2.560 nm, corresponding to few-layer graphene.

The microstructure of the graphene prepared by oxygen-aided CVD was probed by high-resolution transmission electron microscopy (HRTEM), selected-area electron diffraction (SAED), scanning tunneling microscopy (STM), and X-ray photoelectron spectroscopy (XPS). These techniques provide important information about graphene as detailed below. After the graphene film was transferred to a copper grid, the layer count on the edges of the images indicated that the film consisted mostly of material with a thickness corresponding to few-layer graphene or less (Figure 2a−c). The selected SAED pattern in Figure 2d displays two sets of hexagonal symmetrical patterns, which may be caused by the grain boundary or a two-layer graphene with an AB stacking structure.[13,14] The STM image shows the atomic resolution of the graphene lattice on the $SiO_2$/Si substrate (Figure 2e), and the XPS C 1s core-level spectrum shows the characteristic signals of graphene (Figure 2f).[15] The Si 2p binding energy is ∼105.1 eV, which corresponds to $SiO_2$ (inset). As shown by the full XPS spectrum (Figure S3), there were no other signals due to Fe, Co, Ni, Cu, or other metals, confirming that graphene can be synthesized on $SiO_2$ in the absence of metals.[10] All these data indicate that the films had high quality despite the fact that no metal catalysts were employed during graphene growth.

The quality of the graphene on $SiO_2$/Si produced by oxygen-aided CVD was further evaluated using Raman spectroscopy. The spectra reveal the presence of G, 2D, and D bands (Figure 2g). The G band is the result of first-order scattering of the $E_{2g}$ mode observed for $sp^2$ carbon domains,[16] and the 2D band is the most prominent feature in the Raman spectra of high-quality graphene. The shape of the 2D band and the ratio of its intensity relative to that of the G band ($I_G/I_{2D}$) are well-established characteristics of graphene layers.[4] In the case of single-layer graphene, the G and 2D bands were observed at about 1592 and 2793 $cm^{-1}$, respectively. The 2D peak could be fitted by a symmetric sharp peak with $I_G/I_{2D}$ < 0.3, which is characteristic of monolayer graphene. The full width at half-maximum (fwhm) of the 2D peak for our monolayer graphene was 45 ± 5 $cm^{-1}$. The broadening can be explained by a non-uniform number of layers: a small fraction of bi- or few-layer graphene broadens the 2D peak.[17] The 2D bands also become broader with increasing layer number because of the change in the electronic structure of graphene, which affects the process of double resonance.[18] The low intensity of the D peak located at ∼1350 $cm^{-1}$ is consistent with a slight disorder of the graphene layer or may be caused by domain boundaries. The blue shifts of the D, G, and 2D bands of monolayer graphene with respect to those of reported graphene mainly derive from the strong compressive strain effect of the $SiO_2$/Si substrate, although the frequency of the G and 2D Raman bands is also adjusted by charge doping through electron−phonon coupling changes.[19,20] Similar blue shifts were also observed by Ni et al.[21] after thermal annealing of graphene covered with a layer of $SiO_2$: the D, G, and


dx.doi.org/10.1021/ja2063633 |J. Am. Chem. Soc. 2011, 133, 17548–17551

2D bands shifted to higher frequency with an increase in annealing temperature as a result of the strong interaction between graphene and $SiO_2$.

Polycrystalline graphene can also be synthesized on quartz via a similar CVD process (1100 °C, $CH_4$:$H_2$:Ar = 13.5:50:70 sccm; Figure 3). The optical properties of the continuous graphene films formed on quartz were characterized by UV−vis spectroscopy. Figure 3d shows the transmittance spectra of the graphene films, which have high transmittance in the visible and near-IR regions. At a wavelength of 550 nm, the transmittance of the thinnest graphene film was ∼91.2%, and its sheet resistance was ∼800 Ω/□. The transmittance and sheet resistance both decreased with increasing deposition time (Figure 3d). The minimum sheet resistance reached ∼210 Ω/□, and this film had a transmittance of 63.5%. Figure 3e shows a comparison of the sheet resistance of our graphene films with those of previously reported graphene as a function of transmittance at 550 nm. The sheet resistance of graphene formed by oxygen-aided CVD was lower than those of catalyst-free nanographene,[7] chemically reduced graphene oxide,[22] and Ni-catalyzed graphene[5] and close to that of wet-transferred graphene[23] with comparable transmittance. The better optical and electrical properties are attributed to the direct growth process, which avoids the complex postsynthesis transfer process with its associated problems of contamination and film breakage. Bae et al.[24] report that roll-to-roll graphene films have sheet resistances as low as ∼125 Ω/□ with 97.4% optical transmittance, indicating that there is still a room for improving the quality of the graphene grown by oxygen-aided CVD for use in transparent conducting electrode applications. Nevertheless, the oxygen-aided CVD approach simplifies the processing technology, and the current properties meet the requirements for practical applications in electrostatic dissipation, cathode ray tubes, and touch screens.[25]

It has been proposed that the CVD growth of graphene on Ni occurs by a carbon precipitation process,[26] whereas graphene grows on Cu by a different surface-catalyzed process.[27] Therefore, it is of interest to investigate the mechanism of the growth of graphene on $SiO_2$ in the absence of a metal catalyst. According to reported studies of SWCNT growth on nanosized $SiO_2$ particles,[11] the synthesis of graphene on $SiO_2$ substrates involves a vapor−solid−solid (VSS) growth mechanism. We found that heat treatment of the $SiO_2$ substrate in air increased the number of graphene nucleation sites in the subsequent CVD growth (Figure S4). Similar to metal-catalyst-free SWCNT growth, the presence of oxygen can enhance the capture of $CH_x$ ($x$ = 0−4) fragments through C−O and H−O binding and thus provide more opportunities for C−C coupling and graphene nucleation. The graphene growth law also suggests that the oxygen-aided growth is a surface deposition process with a very low reaction rate (1−5 nm/min). Notably, as in the case of graphene grown on Ni or Cu, the growth of microscale graphene sheets needs only a few minutes. According to studies of the role of kinetic factors in graphene growth on Cu,[27] the relative sizes of the mass transport coefficients ($h_g$) and surface reaction constants ($K_s$) influence the growth of graphene: uniform growth of single-layer graphene occurs when $h_g \gg K_s$, and nonuniform growth occurs when $h_g \ll K_s$. A relatively low value of $K_s$ may be the reason for our observed growth of large-scale monolayer rounded graphene sheets on $SiO_2$ in the first period. We also conducted Fourier transform IR (FTIR) spectroscopy, low-angle (30°) XPS, and Raman investigations (Figures S5−S7). A weak SiC signal was detected in graphene samples on quartz, which has

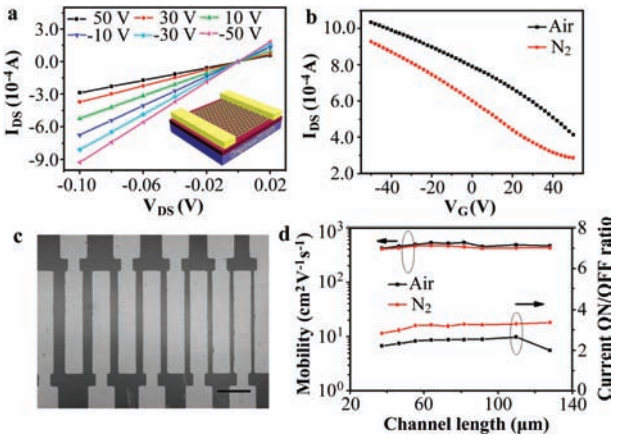


**Figure 4.** Room-temperature oxygen-aided CVD-grown graphene-film FETs. (a) $I_{DS}$−$V_{DS}$ characteristics for a device with a channel length of ∼65 μm and channel width of ∼1200 μm in $N_2$. As $V_G$ was varied from 50 to −50 V, the conductance of the device increased, indicative of a p-type semiconductor. The inset shows a schematic diagram of this device. (b) Transfer characteristics ($I_{DS}$ vs $V_G$) of the graphene device at $V_{DS}$ = 0.1 V in air (black) and $N_2$ (red). (c) SEM image of film FETs with different channel lengths. Scale bar = 400 μm. (d) Mobility and current ON/OFF ratio as a function of channel length in air (black) and $N_2$ (red).

a higher surface roughness than $SiO_2$/Si (Figures 1b and 3a). Bachmatiuk et al.[28] reported the formation of SiC from $SiO_2$ nanoparticles via the carbon thermal reduction.[29] Thus, we think that the nanosized $SiO_2$ risings and carbon nanoparticles formed concomitantly with the growth of graphene probably induce the formation of few-layer graphene (Figures 1e,f and 3b).[28,30,31] The growth mechanism still remains an active area of theoretical and experimental research, and further detailed studies are underway in our laboratory.

To evaluate further the electronic quality of our graphene film, field-effect transistors (FETs) were fabricated on a $SiO_2$/Si wafer with Au as source and drain electrodes and a doped silicon substrate as the back gate. In Figure 4a, typical $I$−$V$ characteristics for a device with a channel length ($L$) of ∼65 μm and a channel width ($W$) of ∼1200 μm in $N_2$ reveal typical hole transport behavior, with a rapid increase in the source−drain current ($I_{DS}$) with increasingly negative gate voltage ($V_G$). The transfer curves of the device are shown in Figure 4b. The $I_{DS}$ value increases monotonically with decreasing $V_G$, indicative of p-type behavior with the neutrality point moved to positive $V_G$.[1] Although vacuum treatment (2 days) caused a shift, in $N_2$ the devices did not exhibit the ambipolar characteristics of graphene FETs because of the strong doping of the substrate. This is also reflected in the blue shift of the G band in the Raman spectra (see Figure 2g). The estimated current "ON/OFF" ratios were about 2.51 in air and 3.24 in $N_2$, which are high values for pure graphene-film-based FET devices. The carrier mobilities calculated from the linear regime of the transfer characteristics are about 531 $cm^2\ V^{-1}\ s^{-1}$ in air and 472 $cm^2\ V^{-1}\ s^{-1}$ in $N_2$. The values are better than those obtained using chemically reduced graphene oxide films (∼1 $cm^2\ V^{-1}\ s^{-1}$, $L$ = 21 μm, $W$ = 400 μm)[3] and also compare favorably with that of PMMA-derived graphene on Cu (∼410 $cm^2\ V^{-1}\ s^{-1}$, $L \approx 7.5$ μm, $W \approx 9$ μm).[32] All of the FET devices in our experiments (Figure 4c,d) showed uniform characteristics regardless of channel length

($L = 30-130\,\mu$m, $W \approx 1200\,\mu$m), confirming the high quality of our graphene films.

In summary, we have developed an oxygen-aided CVD process for synthesizing high-quality polycrystalline graphene on a large scale. Graphene can be directly synthesized on $SiO_2$/Si or quartz, which can be directly incorporated into electronic devices, thus avoiding a complex and skilled postsynthesis transfer process with its associated problems of contamination and film breakage. Our work provides an alternative method for producing graphene on dielectric substrates without matched crystal structure and lattice parameters as well as high-quality samples for a study of the growth mechanism. Unlike metal-catalyzed CVD growth and SiC epitaxial growth, the method presented here is more compatible with current Si processing techniques for fabrication of electronic devices.

## ■ ASSOCIATED CONTENT

**Supporting Information.** Experimental procedures and additional figures. This material is available free of charge via the Internet at http://pubs.acs.org.).

## ■ AUTHOR INFORMATION

**Corresponding Author**
liuyq@iccas.ac.cn

## ■ ACKNOWLEDGMENT

We thank Xu Zhang, Xuanyun Wang, Chongan Di, Changhui Ye, and Hongtao Liu for their assistance with STM characterization and device fabrication. This work was supported by the National Natural Science Foundation of China (60736004, 60911130231), the National Major State Basic Research Development Program (2011CB808403, 2011CB932303, 2009CB623603, 2011CB932701), and the Chinese Academy of Sciences.

## ■ REFERENCES

(1) Novoselov, K. S.; Geim, A. K.; Morozov, S. V.; Jiang, D.; Zhang, Y.; Dubonos, S. V.; Grigorieva, I. V.; Firsov, A. A. *Science* **2004**, *306*, 666.

(2) Berger, C.; Song, Z.; Li, X.; Wu, X.; Brown, N.; Naud, C.; Mayou, D.; Li, T.; Hass, J.; Marchenkov, A. N.; Conrad, E. H.; First, P. N.; de Heer, W. A. *Science* **2006**, *312*, 1191.

(3) Eda, G.; Fanchini, G.; Chhowalla, M. *Nat. Nanotechnol.* **2008**, *3*, 270.

(4) (a) Reina, A.; Jia, X.; Ho, J.; Nezich, D.; Son, H.; Bulovic, V.; Dresselhaus, M. S.; Kong, J. *Nano Lett.* **2009**, *9*, 30. (b) Di, C.; Wei, D.; Yu, G.; Liu, Y.; Guo, Y.; Zhu, D. *Adv. Mater.* **2008**, *20*, 3289. (c) Wei, D.; Liu, Y.; Zhang, H.; Huang, L.; Wu, B.; Chen, J.; Yu, G. *J. Am. Chem. Soc.* **2009**, *131*, 11147. (d) Wu, B.; Geng, D.; Guo, Y.; Huang, L.; Xue, Y.; Zheng, J.; Chen, J.; Yu, G.; Liu, Y.; Jiang, L.; Hu, W. *Adv. Mater.* **2011**, *23*, 3522.

(5) Kim, K. S.; Zhao, Y.; Jang, H.; Lee, S. Y.; Kim, J. M.; Kim, K. S.; Ahn, J. H.; Kim, P.; Choi, J. Y.; Hong, B. H. *Nature* **2009**, *457*, 706.

(6) Li, X.; Cai, W.; An, J.; Kim, S.; Nah, J.; Yang, D.; Piner, R.; Velamakanni, A.; Jung, I.; Tutuc, E.; Banerjee, S. K.; Colombo, L.; Ruoff, R. S. *Science* **2009**, *324*, 1312.

(7) Zhang, L.; Shi, Z.; Wang, Y.; Yang, R.; Shi, D.; Zhang, G. *Nano Res.* **2011**, *4*, 315.

(8) Rümmeli, M. H.; Bachmatiuk, A.; Scott, A.; Borrnert, F.; Warner, J. H.; Hoffman, V.; Lin, J. H.; Cuniberti, G.; Büchner, B. *ACS Nano* **2010**, *4*, 4206.

(9) Hackley, J.; Ali, D.; DiPasquale, J.; Demaree, J. D.; Richardson, C. J. K. *Appl. Phys. Lett.* **2009**, *95*, No. 133114.

(10) Huang, S.; Cai, Q.; Chen, J.; Qian, Y.; Zhang, L. *J. Am. Chem. Soc.* **2009**, *131*, 2094.

(11) Liu, B.; Tang, D. M.; Sun, C.; Liu, C.; Ren, W.; Li, F.; Yu, W. J.; Yin, L. C.; Zhang, L.; Jiang, C.; Cheng, H. M. *J. Am. Chem. Soc.* **2011**, *133*, 197.

(12) Choi, H. M.S. Thesis, University of Massachusetts Lowell, Lowell, MA, 2008; UMI no. 1458539.

(13) Kim, K.; Lee, Z.; Regan, W.; Kisielowski, C.; Crommie, M. F.; Zettl, A. *ACS Nano* **2011**, *5*, 2142.

(14) Liu, N.; Fu, L.; Dai, B.; Yan, K.; Liu, X.; Zhao, R.; Zhang, Y.; Liu, Z. *Nano Lett.* **2011**, *11*, 297.

(15) Nikitin, A.; Näslund, L.; Zhang, Z.; Nilsson, A. *Surf. Sci.* **2008**, *602*, 2575.

(16) Nemanich, R. J. *Phys. Rev. B* **1979**, *20*, 392.

(17) Lee, D. S.; Riedl, C.; Krauss, B.; Klitzing, K.; Starke, U.; Smet, J. H. *Nano Lett.* **2008**, *8*, 4320.

(18) Ni, Z. H.; Wang, H. M.; Kasim, J.; Fan, H. M.; Yu, T.; Wu, Y. H.; Feng, Y. P.; Shen, Z. X. *Nano Lett.* **2007**, *7*, 2758.

(19) Yan, J.; Zhang, Y.; Kim, P.; Pinczuk, A. *Phys. Rev. Lett.* **2007**, *98*, No. 166802.

(20) Pisana, S.; Lazzeri, M.; Casiraghi, C.; Novoselov, K. S.; Geim, A. K.; Ferrari, A. C.; Mauri, F. *Nat. Mater.* **2007**, *6*, 198.

(21) Ni, Z. H.; Wang, H. M.; Ma, Y.; Kasim, J.; Wu, Y. H.; Shen, Z. X. *ACS Nano* **2008**, *2*, 1033.

(22) Zhao, J.; Pei, S.; Ren, W.; Gao, L.; Cheng, H. M. *ACS Nano* **2010**, *4*, 5245.

(23) Li, X.; Zhu, Y.; Cai, W.; Borysiak, M.; Han, B.; Chen, D.; Piner, R. D.; Colombo, L.; Ruoff, R. S. *Nano Lett.* **2009**, *9*, 4359.

(24) Bae, S.; et al. *Nat. Nanotechnol.* **2010**, *5*, 574.

(25) Kaempgen, M.; Duesberg, G. S.; Roth, S. *Appl. Surf. Sci.* **2005**, *252*, 425.

(26) Li, X.; Cai, W.; Colombo, L.; Ruoff, R. S. *Nano Lett.* **2009**, *9*, 4268.

(27) Bhaviripudi, S.; Jia, X.; Dresselhaus, M. S.; Kong, J. *Nano Lett.* **2010**, *10*, 4128.

(28) Bachmatiuk, A.; Borrnert, F.; Grobosch, M.; Schaffel, F.; Wolff, U.; Scott, A.; Zaka, M.; Warner, J. H.; Klingeler, R.; Knupfer, M.; Buchner, B.; Rummeli, M. H. *ACS Nano* **2009**, *3*, 4098.

(29) Vix-Gutesrl, C.; Ehrburger, P. *Carbon* **1997**, *35*, 1587.

(30) Takagi, D.; Kobayashi, Y.; Homma, Y. *J. Am. Chem. Soc.* **2009**, *131*, 6922.

(31) Yao, Y.; Feng, C. Q.; Zhang, J.; Liu, Z. F. *Nano Lett.* **2009**, *9*, 1673.

(32) Sun, Z.; Yan, Z.; Yao, J.; Beitler, E.; Zhu, Y.; Tour, J. M. *Nature* **2010**, *468*, 549.